Unsupervised Mammograms Segmentation

Michal Haindl   Stanislav Mikeš

Institute of Information Theory and Automation
of the ASCR, 182 08 Prague, Czech Republic
{haindl,xaos}@utia.cz

Abstract

We present a multiscale unsupervised segmenter for automatic detection of potentially cancerous regions of interest containing fibroglandular tissue in digital screening mammography. The mammogram tissue textures are locally represented by four causal multispectral random field models recursively evaluated for each pixel and several scales. The segmentation part of the algorithm is based on the underlying Gaussian mixture model and starts with an over segmented initial estimation which is adaptively modified until the optimal number of homogeneous mammogram segments is reached. The performance of the presented method is verified on the Digital Database for Screening Mammography (DDSM) from the University of South Florida as well as extensively tested on the Prague Texture Segmentation Benchmark and compares favourably with several alternative unsupervised texture segmentation methods.

1. Introduction

Breast cancer is the leading cause of death [17, 15] among all cancers for middle-aged women in most developed countries. Thus a significant effort is currently focused on cancer prevention and early detection which can substantially reduce the mortality rate. X-ray screening mammography is the most frequented method for breast cancer early detection although not without problems [15] such as rather large minimum detectable tumor size, higher mammogram sensitivity for older women or radiation exposition. Automatic mammogram analysis is still difficult task due to wide variation of breast anatomy, nevertheless a computer-aided diagnosis system can successfully assist a radiologist, and can be used as a second opinion. The first step in a such system is detection of suspicious potentially cancerous regions of interest . Several approaches to detect these regions of interest (ROI) were published [17], mostly

based on supervised learning. We propose an unsupervised segmentation method for fast automatic mammogram segmentation into the regions of interest (ROI) using a statistical random field based texture representation. The presented method detects the fibroglandular tissue regions from either craniocaudal (CC) or mediolateral oblique (MLO) views and thus can help focus a radiologist to this most important breast region. Spatial interaction models and especially Markov random fields-based models are increasingly popular for texture representation [10, 16, 5], etc. Several researchers dealt with the difficult problem of unsupervised segmentation using these models see for example [12, 14, 1], or [7], which is also addressed in this paper.

2. Breast Detector

The method starts with automatic breast area detection because it can be easily computed and simplifies the subsequent fibroglandular tissue region detection. This is performed using simple histogram thresholding with an automatically selected threshold. In this step the method also recognizes several label areas on a mammogram. We compute their areas and all but the largest one are discarded and merged with the background. In this stage the algorithm also decides the breast orientation (left or right) on the mammogram. Fig. 1 -breast mask illustrates the resulting detected breast area (in inverted grey levels). The following detection of regions of interest is performed only in the breast region ignoring the background area set in the mask template.

3. Breast Tissue Texture Model

Our method segments pseudo-colour multiresolution mammograms each created from the original greyscale mammogram and its two nonlinear gamma transformations. We assume to down-sample input image Y into $M = 3$ different resolutions $Y^{(m)} = \downarrow^{\iota_m} Y$ with sampling factors $\iota_m \quad m = 1, \ldots, M$ identical for both

B-3056-1 right CC

breast mask

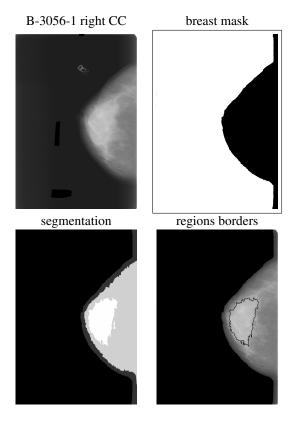segmentation

regions borders

Figure 1. Normal right breast mammogram (patient age 58, but with a cancerous lesion in the left breast), the detected breast area, segmentation result and detected regions of interest, respectively.

directions and $Y^{(1)} = Y$. Local texture for each pixel $Y_r^{(m)}$ is represented using the 3D CAR model parameter space $\Theta_r^{(m)}$. The concept of decision fusion [11] for high-performance pattern recognition is well known and widely accepted in the area of supervised classification where (often very diverse) classification technologies, each providing complementary sources of information about class membership, can be integrated to provide more accurate, robust and reliable classification decisions than the single classifier applications. The proposed method circumvents the problem of multiple unsupervised segmenters combination [6] by fusing multiple-processed measurements into a single segmenter feature vector.

Smooth pseudo-colour mammogram textures require three dimensional models for adequate representation. We assume that single multi spectral texture can be locally modeled using a 3D simultaneous causal autoregressive random field model (CAR). This model can

be expressed as a stationary causal uncorrelated noise driven 3D autoregressive process [8]:

$$Y_r = \gamma X_r + e_r \quad , \qquad (1)$$

where $\gamma = [A_1, \ldots, A_\eta]$ is the $3 \times 3\eta$ parameter matrix, e_r is a white Gaussian noise vector with zero mean and a constant but unknown variance, X_r is a corresponding vector of the contextual neighbours Y_{r-s} and $r, r-1, \ldots$ is a chosen direction of movement on the image index lattice I. $\eta = card(I_r^c)$ where I_r^c is a causal neighborhood index set (e.g. $I_r^c = \{(r_1, r_2 - 1), (r_1 - 1, r_2)\}$). The optimal neighbourhood (I_r^c) as well as the Bayesian parameters estimation of a CAR model can be found analytically under few additional and acceptable assumptions using the Bayesian approach [8]. The recursive Bayesian parameter estimation of the CAR model is [8]:

$$\hat{\gamma}_{r-1}^T = \hat{\gamma}_{r-2}^T + \frac{V_{x(r-2)}^{-1} X_{r-1}(Y_{r-1} - \hat{\gamma}_{r-2} X_{r-1})^T}{(1 + X_{r-1}^T V_{x(r-2)}^{-1} X_{r-1})} \quad ,$$

where $V_{x(r-1)} = \sum_{k=1}^{r-1} X_k X_k^T + V_{x(0)}$. Each matrix contains local estimations of the CAR model parameters. These models have identical contextual neighbourhood I_r^c but they differ in their major movement direction (top-down, bottom-up, rightward, leftward). The local texture for each pixel and M resolutions $\alpha_1, \ldots, \alpha_M$ is represented by four parametric matrices t, b, r, l e.g. $\hat{\gamma}_r^{i,\alpha_j}$ for $i \in \{t, b, r, l\}$, $j = 1, \ldots, M$ which are subsequently compressed using the local PCA (for computational efficiency) into $\tilde{\gamma}_r^{i,\alpha_j}$. Single resolution compressed parameters are composed into M parametric matrices:

$$\tilde{\gamma}_r^{\alpha_j \, T} = \{\tilde{\gamma}_r^{t,\alpha_j}, \tilde{\gamma}_r^{b,\alpha_j}, \tilde{\gamma}_r^{r,\alpha_j}, \tilde{\gamma}_r^{l,\alpha_j}\}^T \, j = 1, \ldots, M \quad .$$

The parametric space $\tilde{\gamma}^{\alpha_j}$ is subsequently smooth out, rearranged into a vector and its dimensionality is reduced using the PCA feature extraction ($\bar{\gamma}^{\alpha_j}$). Finally we add the average local spectral values $\zeta_r^{\alpha_j}$ to the resulting feature vector:

$$\Theta_r = [\bar{\gamma}_r^{\alpha_1}, \zeta_r^{\alpha_1}, \ldots, \bar{\gamma}_r^{\alpha_M}, \zeta_r^{\alpha_M}]^T \quad . \qquad (2)$$

Rough scale pixels parameters are simply mapped to the corresponding fine scale locations.

4. Texture Parametric Space Segmentation

Multi-spectral, multiresolution texture segmentation is done by clustering in the combined CAR models parameter space Θ defined on the lattice I where Θ_r is

the modified parameter vector (2) computed for the lattice location r. We assume that this parametric space can be represented using the Gaussian mixture model (GM) with diagonal covariance matrices due to the previous CAR parametric space decorrelation. The Gaussian mixture model for CAR parametric representation is as follows:

$$p(\Theta_r) \quad = \quad \sum_{i=1}^{K} p_i \, p(\Theta_r \,|\, \nu_i, \Sigma_i) \ , \qquad (3)$$

$$p(\Theta_r \,|\, \nu_i, \Sigma_i) \quad = \quad \frac{|\Sigma_i|^{-\frac{1}{2}}}{(2\pi)^{\frac{d}{2}}} \, e^{-\frac{(\Theta_r - \nu_i)^T \Sigma_i^{-1}(\Theta_r - \nu_i)}{2}} \quad (4)$$

The mixture model equations (3),(4) are solved using a modified EM algorithm. The algorithm is initialized using ν_i, Σ_i statistics estimated from the corresponding regions obtained by regular division of the input detected breast area. An alternative initialization can be random choice of these statistics. For each possible couple of regions the Kullback Leibler divergence

$$D\left(p(\Theta_r \,|\, \nu_i, \Sigma_i) \,||\, p(\Theta_r \,|\, \nu_j, \Sigma_j)\right) =$$

$$\int_{\Omega} p(\Theta_r \,|\, \nu_i, \Sigma_i) \, \log\left(\frac{p(\Theta_r \,|\, \nu_i, \Sigma_i)}{p(\Theta_r \,|\, \nu_j, \Sigma_j)}\right) \, d\Theta_r \qquad (5)$$

is evaluated and the most similar regions, i.e.,

$$\{i, j\} = \arg\min_{k,l} D\left(p(\Theta_r \,|\, \nu_l, \Sigma_l) \,||\, p(\Theta_r \,|\, \nu_k, \Sigma_k)\right)$$

are merged together in each step. This initialization results in K_{ini} subimages and recomputed statistics ν_i, Σ_i. $K_{ini} > K$ where K is the optimal number of textured segments to be found by the algorithm. Two steps of the EM algorithm are repeating after the initialization. The components with smaller weights than a fixed threshold ($p_j < \frac{0.01}{K_{ini}}$) are eliminated. For every pair of components we estimate their Kullback Leibler divergence (5). From the most similar couple, the component with the weight smaller than the threshold is merged to its stronger partner and all statistics are actualized using the EM algorithm. The algorithm stops when either the likelihood function has negligible increase ($\mathcal{L}_t - \mathcal{L}_{t-1} < 0.01$) or the maximum iteration number threshold is reached.

The parametric vectors representing texture mosaic pixels are assigned to the clusters according to the highest component probabilities, i.e., Y_r is assigned to the cluster ω_{j*} if

$$\pi_{r,j*} = max_j \sum_{s \in I_r} w_s \, p(\Theta_{r-s} \,|\, \nu_j, \Sigma_j) \ ,$$

where w_s are fixed distance-based weights, I_r is a rectangular neighbourhood and $\pi_{r,j*} > \pi_{thre}$ (otherwise the pixel is unclassified). The area of single cluster blobs is evaluated in the post-processing thematic
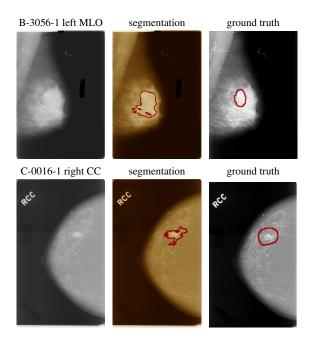

Figure 2. Cancerous mammograms (patients age 58 (top) and 80 (bottom)), radiologist associated ground truth and detected regions of interest using the multiple segmenter approach, respectively.

map filtration step. Regions with similar statistics are merged. Thematic map blobs with area smaller than a given threshold are attached to its neighbour with the highest similarity value. Finally, regions which have grey level mean value difference from the median mean value (over the same type of digitized mammograms) of cancerous ground truth regions larger than a specified threshold are eliminated.

5. Experimental Results

The algorithm was tested on mammograms from the Digital Database for Screening Mammography (DDSM) from the University of South Florida [9]. This database contains 2620 four view (left and right craniocaudal (CC) and mediolateral oblique (MLO)) mammograms in different resolutions. Single mammograms cases are divided into normal, benign, benign without callback volumes and cancer. All our experiments are done with three resolutions ($M = 3$) using sampling factors $\iota_1 = 2, \iota_2 = 4, \iota_3 = 8$ and the causal neighbourhood with fourteen neighbours ($\eta = 14$). Fig. 2-top show left MLO mammogram of a patient age 58 with detected malignant asymmetric lesion and the

right CC mammogram (Fig. 2-bottom) of a patient age 80 with detected irregular, spiculated malignant lesion type. The segmenter correctly found the region of interest with the cancer lesion on both mammograms. The detected region of interest results Figs. 1-2 demonstrate very good region segmentation and low over-segmentation properties of our method. The general segmentation part of our method (without mammography specific steps) was also successfully numerically compared [6] with several alternative algorithms JSEG [4], Blobworld [2], GMRF-GM [7] and Edison [3]. These algorithms on the Prague Texture Benchmark [7, 13] performed steadily worse as can be seen in the [6] or on the benchmark web (http://mosaic.utia.cas.cz). For all the 27 benchmark criteria our method is either the best one or the next best with marginal difference from the best one. Resulting ROI segmentation results are promising however comparison with other algorithms is difficult because of lack of sound experimental evaluation results in the field of screening mammography segmentation.

6. Conclusions

We proposed the efficient method for completely automatic unsupervised detection of mammogram fibroglandular tissue regions of interest. This method is based on the underlying 3D CAR and GM texture models. Although our algorithm uses Markovian models it is fast due to robust recursive models parameter estimation and therefore it is much faster than usual Markovian approaches which often require time consuming iterative Markov chain Monte Carlo methods to estimate their parameters. Usual drawback of segmentation methods are many application dependent parameters to be experimentally estimated. Our method requires only a contextual neighbourhood selection and two additional thresholds. The algorithm's performance is favourably demonstrated on the extensive benchmark tests on large screening mammography database and also natural texture mosaics Prague benchmark ([6, 13]), where it outperforms several alternative segmenters.

Acknowledgements

References

[1] P. Andrey and P. Tarroux. Unsupervised segmentation of markov random field modeled textured images using selectionist relaxation. *IEEE Trans. on PAMI*, 20(3):252–262, March 1998.

[2] C. Carson, M. Thomas, S. Belongie, J. M. Hellerstein, and J. Malik. Blobworld: A system for region-based image indexing and retrieval. In *Third International Conference on Visual Information Systems*. Springer, 1999.

[3] C. Christoudias, B. Georgescu, and P. Meer. Synergism in low level vision. In R. Kasturi, D. Laurendeau, and C. Suen, editors, *Proceedings of the 16th Int. Conf. on Pattern Recognition*, volume 4, pages 150–155, Los Alamitos, August 2002. IEEE Computer Society.

[4] Y. Deng and B. Manjunath. Unsupervised segmentation of color-texture regions in images and video. *IEEE Trans. on PAMI*, 23(8):800–810, August 2001.

[5] M. Haindl. Texture synthesis. *CWI Quarterly*, 4(4):305–331, December 1991.

[6] M. Haindl and S. Mikes. Unsupervised texture segmentation using multiple segmenters strategy. In M. Haindl, J. Kittler, and F. Roli, editors, *MCS 2007*, volume 4472 of *LNCS*, pages 210–219. Springer, 2007.

[7] M. Haindl and S. Mikeš. Model-based texture segmentation. *Lecture Notes in Computer Science*, (3212):306 – 313, 2004.

[8] M. Haindl and S. Šimberová. *Theory & Applications of Image Analysis*, chapter A Multispectral Image Line Reconstruction Method, pages 306–315. World Scientific Publishing Co., Singapore, 1992.

[9] M. Heath, K. Bowyer, D. Kopans, R. Moore, and P. Kegelmeyer. The digital database for screening mammography. In *Proc. of the 5th Int. Workshop on Digital Mammography*. Medical Physics Publishing, 2000.

[10] R. Kashyap. Image models. In K. F. T.Y. Young, editor, *Handbook of Pattern Recognition and Image Processing*. Academic Press, New York, 1986.

[11] J. Kittler, A. Hojjatoleslami, and T. Windeatt. Weighting factors in multiple expert fusion. In *Proc. BMVC*, pages 41–50. BMVA, BMVA, 1997.

[12] B. Manjunath and R. Chellapa. Unsupervised texture segmentation using markov random field models. *IEEE Trans. on PAMI*, 13:478–482, 1991.

[13] S. Mikeš and M. Haindl. Prague texture segmentation data generator and benchmark. *ERCIM News*, (64):67–68, 2006.

[14] D. Panjwani and G. Healey. Markov random field models for unsupervised segmentation of textured color images. *IEEE Transactions on Pattern Analysis and Machine Intelligence*, 17(10):939–954, 1995.

[15] H. Qi and N. A. Diakides. Thermal infrared imaging in early breast cancer detection - a survey of recent research. In *25th Annual Int. Conference of the IEEE EMBS*, pages 448–452, 2003.

[16] T. R. Reed and J. M. H. du Buf. A review of recent texture segmentation and feature extraction techniques. *CVGIP–Image Understanding*, 57(3):359–372, May 1993.

[17] T. Tweed and S. Miguet. Automatic detection of regions of interest in mammographies based on a combined analysis of texture and histogram. In *ICPR*, volume 02, pages 448–452, Los Alamitos, CA, USA, 2002. IEEE Computer Society.